Quadrotor Guidance-Control for flight like nonholonomic vehicle system

Yasser Bouzid, Yasmina Bestaoui, Houria Siguerdidjane, Mehdi Zareb

Quadrotor Guidance-Control for flight like nonholonomic vehicles

Yasser BOUZID[1], Yasmina BESTAOUI[1], Houria SIGUERDIDJANE[2], and Mehdi ZAREB[3]

Abstract— **This paper introduces a velocity based guidance strategy for 3D time-prescribed path following. A second alternative, acceleration based guidance law that incorporates an integral action, is proposed to deal with the more adverse environments. The proposed strategy, which is combined with an efficient nonlinear control strategy for under-actuated systems, is applied to a quadrotor. It ensures the convergence toward the reference trajectory and allows the quadrotor to imitate the behavior of a fixed-wing UAV in the plane (non-holonomic like-navigation). The effectiveness of the proposed Guidance & Control (G&C) loop is shown through some numerical simulations.**

I. INTRODUCTION

Nowadays, a broad range of studies treating the Guidance and Control (G&C) of autonomous systems especially for the Miniature-Unmanned Aerial Vehicles (MUAVs) have been published. These two loops (G&C) are necessary to achieve any mission properly as for instance the monitoring of structures [1], the coverage [2], etc.

The guidance loop provides the reference signals (angles, velocities, etc.) required by the flight controller. It ensures many tasks from the trajectory planning [3] to the trajectory generation [4]. The paper [5] presents straight-circular paths following method using vector fields while the reference [4] shows a strategy enabling aggressive maneuvers as well as flying through narrow gaps. In reference [6], the well-known helmsman guidance law has been studied deeply. Extensive other guidance strategies are worth citing but the reader may refer to review papers [7][8] and the references therein for more details.

The quadrotor is a nonlinear, under-actuated and highly coupled system. Thus, various methods have been applied for the trajectory tracking control as well as for the attitude stabilization. The classic linear control strategies operate in particular waypoints and assume a linear model [9]. However, the application of the nonlinear control techniques can improve the performance as shown in [10] [11] [12].

The main objective of the present paper is to imitate a fixed-wing UAV in planar-flight (non-holonomic-like navigation) along a time-parameterized path as well as the tracking of a moving object. These abilities are requested for several applications (inspection, indoor navigation, filming, etc.). In [13], a reactive vision-based autonomous navigation, within an indoor corridor, is performed by a quad-rotor. The dynamic model is divided into two parts considering two planes called Q-plane and R-plane using saturated PD controller. The same problem of navigation is considered in [14] but under the effect of wind.

For non-holonomic navigation, the quadrotor has to satisfy some desired dynamic behavior while tracking the geometric path. Thus, the quadrotor dynamic model is arranged in such a way that the lateral motion (roll rotation) can be canceled. Then, the quadrotor is able to reach any configuration, defined in the space by its absolute position and the yaw angle, using the forward and heading motions. In other words, we employ only the longitudinal flight (pitch rotation), vertical flight and yaw rotation.

The paper addresses the use of virtual body based frame, which is represented by a position variable belonging to the desired path and supposed to move along it at all times. The proposed strategy mixes the construction of the geometric path in space and time assignments. The guidance law ensures that the vehicle converges towards the path in a non-holonomic way involving the velocity vector. This strategy also allows the tracking of a real moving body in the space. Besides, an efficient flight controller based on a nonlinear approach is required. Herein, we apply the Immersion & Invariance (I&I) approach to design the flight controller that ensures an asymptotic stability. The effectiveness of the proposed G&C strategy design is shown through some promising numerical simulations.

The paper is organized as follows: Section II introduces the problem. Section III presents the design of the proposed guidance strategy with an application to the quadrotor. Section IV addresses the design of the flight controller employing the I&I theory. Section V shows some obtained promising numerical results. Finally, a conclusion is drawn in Section VI.

II. PROBLEM STATEMENT

The classic way of quadrotor guidance is to focus on the absolute position of the vehicle without taking care of the velocity vector. Besides the stationary flight capability, the quadrotor is able to perform any trajectory in the space employing the longitudinal and lateral motions where the heading angle is maintained at the origin (see Figure 1 (a)). However, this way of navigation is not recommended for many applications such as: object tracking, movie filming and indoor building inspection (see Figure 2) where the heading and forward motions play a crucial role (e.g. quadrotor with frontal camera). Therefore, we propose a non-holonomic like-navigation way (see Figure 1 (b)).

[1]Y. Bouzid and Y. Bestaoui are with IBISC, Université d'Evry, Université Paris-Saclay, Evry, 91000, France yasseremp@gmail.com, Yasmina.Bestaouisebbane@univ-evry.fr

[2]H. Siguerdidjane is with s with L2S, CentraleSupélec, Université Paris-Saclay, Gif sur yvette, 91190, France Houria.Siguerdidjane@centralesupelec.fr

[3]M. Zareb is with LEPESA Laboratory, Electronic Department, USTO-MB, El Mnaouar, 31000, Algeria

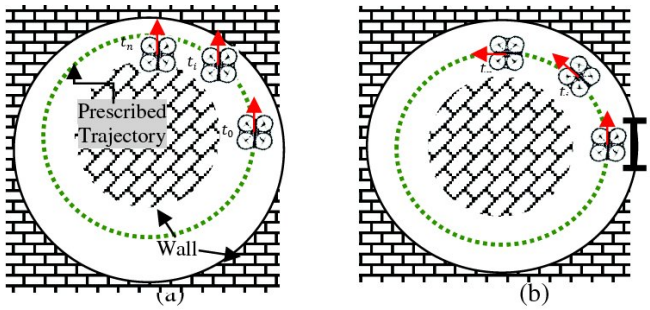

Fig. 1. (a) Classical navigation involving the roll, the pitch and the absolute position of the vehicle. Fig. 1. (b) Fixed wing like-navigation involving the heading angle and the forward motion.

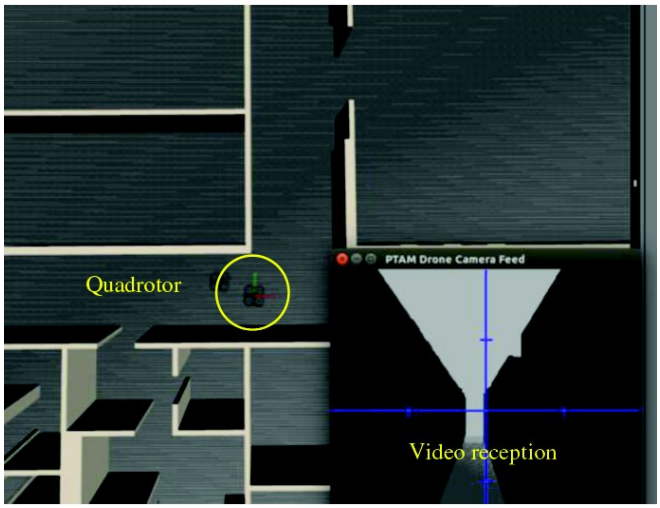

Fig. 2. Indoor building inspection (Gazebo simulator).

Herein, our guidance law is based on the notion of virtual body, which can instantaneously perform any desired motion $P_{ref}(t)$. This latter should take care of the obstacles avoidance and the optimality concerns[1]. It is worthwhile to stress that the proposed guidance law occurs for dynamic tasks. In other words, we seek to make the speed of the real vehicle converges to the desired speed of the virtual vehicle (see Figure 3) and of course it is required that the vehicle, of current absolute position $P(t)$, reaches the time-parameterized path $P_{ref}(t)$ at time t_n . The presence of wind causes erroneous flight trajectory shifting away the vehicle from the preplanned path. Therefore, a second alternative of guidance strategy is proposed to deal with this unfavorable circumstance.

Explicitly, we consider a virtual vehicle $M_v(x_v, y_v, z_v)$ that moves perfectly along a prescribed 3D-path P_{ref} with a forward speed V_v. The real vehicle $M_b(x_b, y_b, z_b)$, which moves with forward speed [2] of magnitude $V_b(> V_0 \geq 0)$,

[1]The optimal path planning with obstacles avoidance is already considered in our previous work and allows generating $P_{ref}(t)$ for the virtual body using Rapidly Random Trees (RRT) strategy [15].

[2]V_0 is the minimal allowed speed. For the fixed wing UAV, $V_0 > 0$ is strictly positive and called stall velocity. It is a necessary condition to avoid the crash of the UAV. However, V_0 may equal zero for the quadrotors (hovering capability).

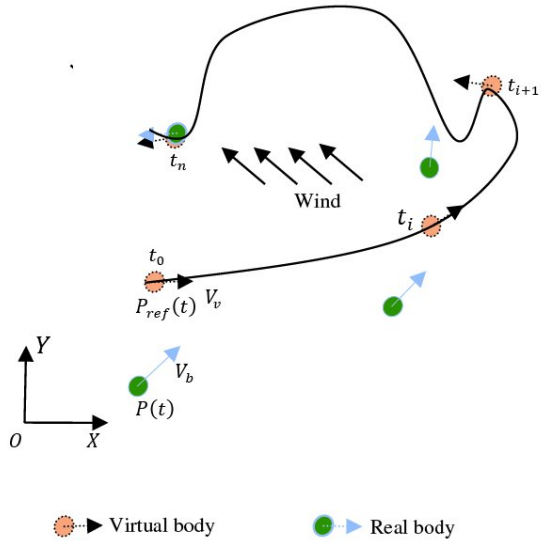

Fig. 3. Virtual body velocity based guidance strategy.

has as focusing task to track the virtual vehicle. In other words, the objective is to ensure identical speeds of vehicles and of course to reduce the tracking error between M_b and M_v. Therefore, three frames are considered that are: the inertial frame $R_0(O_0, X, Y, Z)$, the body-fixed frame noted by $R_1(O_1, X, Y, Z)$ and related to the vehicle center of mass and finally the virtual vehicle frame, $R_v(O_v, T, N, B)$, related to a virtual vehicle where, T is the tangent, N the normal and N the bi-normal. We investigate in this work a guidance law that provides for the flight controller a forward speed V_b, flight path angle denoted by γ and heading angle denoted by χ, which match with the desired forward speed V_v and angles $\gamma_{ref} \neq \pm\frac{\pi}{2}$, $\chi_{ref} \neq \pm\frac{\pi}{2}$ that are related to the virtual vehicle respectively. Let γ_{ref} the angle between the vertical axis Z and the bi-normal axis B and χ_{ref} the angle between the tangent axis T and X (see Figure 4). Thus, the desired reference rotation matrix is

$$R_{ref|3D} = \\ = \begin{bmatrix} \cos(\gamma_{ref})\cos(\chi_{ref}) & \cos(\gamma_{ref})\sin(\chi_{ref}) & -\sin(\gamma_{ref}) \\ -\sin(\chi_{ref}) & \cos(\chi_{ref}) & 0 \\ \sin(\gamma_{ref})\cos(\chi_{ref}) & \sin(\gamma_{ref})\sin(\chi_{ref}) & \cos(\gamma_{ref}) \end{bmatrix}$$

where $R_{ref|3D}$ is orthogonal rotation matrix. The first order time derivative gives

$$\dot{R}_{ref|3D} = S(\gamma_{ref}, \chi_{ref}, \dot{\gamma}_{ref}, \dot{\chi}_{ref}) R_{ref|3D} \quad (1)$$

with $S(\gamma_{ref}, \chi_{ref}, \dot{\gamma}_{ref}, \dot{\chi}_{ref})$ is a skew symmetric matrix written as

$$S(\gamma_{ref}, \chi_{ref}, \dot{\gamma}_{ref}, \dot{\chi}_{ref}) = \\ \begin{bmatrix} 0 & \dot{\chi}_{ref}\cos(\gamma_{ref}) & -\dot{\gamma}_{ref} \\ -\dot{\chi}_{ref}\cos(\gamma_{ref}) & 0 & -\dot{\chi}_{ref}\sin(\gamma_{ref}) \\ \dot{\gamma}_{ref} & \dot{\chi}_{ref}\sin(\gamma_{ref}) & 0 \end{bmatrix}$$

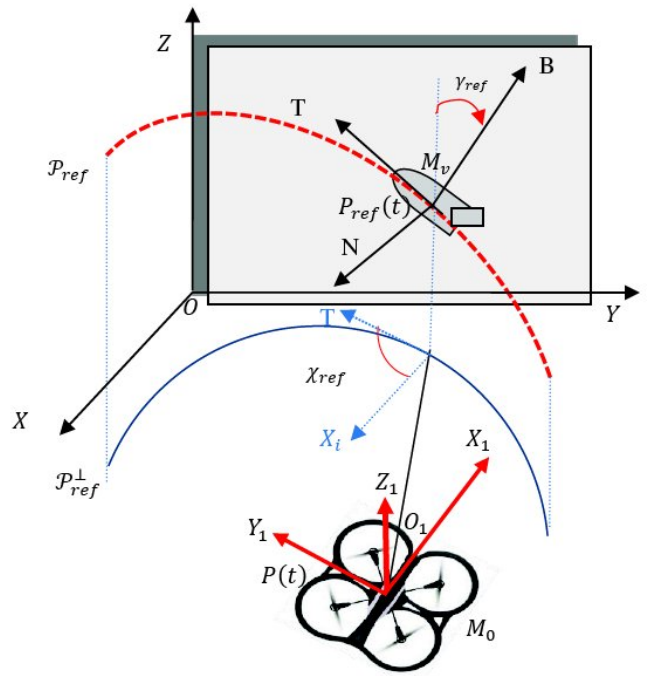

Fig. 4. Frames representation.

III. GUIDANCE LAW

A. Velocity based guidance law

Let

$$\delta(t) = R_{ref|3D}\varepsilon(t) \tag{2}$$

being the position error vector with respect to the frame R_v where $\varepsilon(t)$ denotes the tracking error between the absolute position vector $P(t)$ of the vehicle and the virtual one $P_{ref}(t)$ with respect to the inertial reference frame

$$\varepsilon(t) = P(t) - P_{ref}(t) \tag{3}$$

This error should be converging toward the origin. To deal with this requirement, we impose the first order dynamics of the error expressed in the virtual frame as

$$\dot{\delta}(t) + \lambda_v \delta(t) = 0 \tag{4}$$

where λ_v is a diagonal positive definite matrix that adjusts the speed of convergence.

By differentiating (2) with respect to time and using equation (4) we obtain a new first-order dynamic expressed in the inertial frame as

$$\dot{\varepsilon}(t) + \lambda_i \varepsilon(t) = 0 \tag{5}$$

where

$$\begin{aligned}\lambda_i &= R^{-1}_{ref|3D}(S(\gamma_{ref},\chi_{ref},\dot{\gamma}_{ref},\dot{\chi}_{ref}))R_{ref|3D} + \lambda_v I \\ &= \begin{bmatrix} \lambda_v & \dot{\chi}_{ref} & -\dot{\gamma}_{ref}\cos(\chi_{ref}) \\ -\dot{\chi}_{ref} & \lambda_v & -\dot{\gamma}_{ref}\sin(\chi_{ref}) \\ \dot{\gamma}_{ref}\cos(\chi_{ref}) & \dot{\gamma}_{ref}\sin(\chi_{ref}) & \lambda_v \end{bmatrix}\end{aligned} \tag{6}$$

The velocity error vector in the inertial frame may be written as

$$\dot{\varepsilon}(t) = V - V_{ref} \tag{7}$$

where $V = (V_x, V_y, V_z)^T$ is the vehicle velocity vector and $V_{ref} = (V_{x,ref}, V_{y,ref}, V_{z,ref})^T$ the virtual vehicle velocity vector.

Hence, using (5) and (7), the velocity vector may be expressed as

$$V = -\lambda_i \varepsilon(t) + V_{ref} \tag{8}$$

This last equation needs the computation of matrix (6), which amounts to first calculate the desired reference of the heading and flight path angles γ_{ref} , χ_{ref} together with their time derivatives $\dot{\gamma}_{ref}$, $\dot{\chi}_{ref}$. In tri-dimensional space, the orientation is characterized by:

$$\begin{cases} \chi &= \dfrac{V_y}{|V_y|}\arccos\dfrac{V_x}{\|V\|_2} \\ \gamma &= \arcsin\dfrac{V_z}{V_b} \end{cases} \tag{9}$$

with $\|V\|_2 = \sqrt{V_x^2 + V_y^2}$ and $V_b = \sqrt{V_x^2 + V_y^2 + V_z^2}$

In addition, the first time derivatives are:

$$\begin{cases} \dot{\chi} &= \dfrac{-V_y}{\|V_y\|}\left(\dfrac{a_x V_y - V_x a_y}{\|V\|_2^2}\right) \\ \dot{\gamma} &= \dfrac{a_z\|V\|_2^2 - a_x V_z V_x - a_y V_z V_y}{\|V\|_2} \end{cases} \tag{10}$$

$a = (a_x, a_y, a_z)^T$ denotes the vehicle acceleration vector. Therefore, employing systems (9) and (10) and considering the virtual vehicle, we are able to compute matrix (6).

Remark 1: *As the forward speed is strictly positive ($> V_0$), there is not a problem of singularities at zero for the previous equations.*

B. Quadrotor guidance law application

Since the attitude subsystem is totally decoupled from the altitude dynamics for the quadrotors (see Eqs (20-21))[3], the 3D description for the fixed-wing UAVs becomes a 2D one for the quadrotors. At this stage, the guidance law is synthesized in order to provide the heading angle χ and the speed V_b that go closer to the reference angle χ_{ref} and virtual vehicle speed V_v respectively (no flight path angle, i.e. $\gamma_{ref} = 0$). This means that the altitude reference trajectories are provided independently to those of the attitude angles, unlike the fixed-wing UAV where the altitude trajectories can be described in function of the flight path angle and the forward velocity. Therefore, we consider a projection $P^{\perp}_{ref}$ (2D path) of the 3D-path P_{ref} on the plane XY that should be followed by the quadrotor while the altitude is ensured independently in order to cancel the distance between the desired high and the current altitude of the quadrotor. Thus, we focus on the planar position of the virtual and real vehicles. In other words, $P(t) = (x_b, y_b)^T$, and $P_{ref}(t) = (x_v, y_v)^T$ have herein only two components. Therefore, $R_{ref|3D}$ becomes

$$\begin{aligned} &R_{ref|2D} = \\ &= \begin{bmatrix} \cos(\chi_{ref}) & \sin(\chi_{ref}) \\ -\sin(\chi_{ref}) & \cos(\chi_{ref}) \end{bmatrix} \end{aligned} \tag{11}$$

[3]The opposite is not true i.e. the altitude depends on the attitude angles.

where $R_{ref|2D}$ is orthogonal rotation matrix. Its first-time derivative gives

$$\begin{aligned}\dot{R}_{ref|2D} &= S(\chi_{ref},\dot{\chi}_{ref})R_{ref|2D} \\ &= \begin{bmatrix} -\dot{\chi}_{ref}\sin(\chi_{ref}) & \dot{\chi}_{ref}\cos(\chi_{ref}) \\ -\dot{\chi}_{ref}\cos(\chi_{ref}) & -\dot{\chi}_{ref}\sin(\chi_{ref}) \end{bmatrix}\end{aligned} \tag{12}$$

with $S(\chi_{ref},\dot{\chi}_{ref}) = \begin{bmatrix} 0 & \dot{\chi}_{ref} \\ -\dot{\chi}_{ref} & 0 \end{bmatrix}$ and the second time derivative is

$$\begin{aligned}\ddot{R}_{ref|2D} &= \dot{S}(\chi_{ref},\dot{\chi}_{ref})R_{ref|2D} + S^2(\chi_{ref},\dot{\chi}_{ref})R_{ref|2D} \\ &= \begin{bmatrix} -\ddot{\chi}_{ref}S_{\chi_{ref}} - \dot{\chi}^2_{ref}C_{\chi_{ref}} & \ddot{\chi}_{ref}C_{\chi_{ref}} - \dot{\chi}^2_{ref}S_{\chi_{ref}} \\ -\ddot{\chi}_{ref}C_{\chi_{ref}} + \dot{\chi}^2_{ref}S_{\chi_{ref}} & -\ddot{\chi}_{ref}S_{\chi_{ref}} - \dot{\chi}^2_{ref}C_{\chi_{ref}} \end{bmatrix}\end{aligned} \tag{13}$$

The behavior of the quadrotor in this configuration is similar to the fixed-wing UAV that moves in the plane.

In the case of quadrotor, we follow the same methodology as described above. However, simpler matrix λ_i is obtained

$$\lambda_i = \begin{bmatrix} \lambda_v & \dot{\chi}_{ref} \\ -\dot{\chi}_{ref} & \lambda_v \end{bmatrix} \tag{14}$$

The quadrotor guidance law proposed in (8) exhibits poor capabilities to cancel the steady-state errors. For the sake of improvement, we suppose now that the error has second order dynamics as

$$\ddot{\delta}(t) + \mu_v\dot{\delta}(t) + \alpha_v\delta(t) = 0 \tag{15}$$

where α_v and μ_v are diagonal positive definite matrices that adjust the behavior of convergence.

By two successive time derivatives of (2) and using equations (15) the dynamics of the tracking error expressed in the inertial frame becomes

$$\ddot{\varepsilon}(t) + \mu_i\dot{\varepsilon}(t) + \alpha_i\varepsilon(t) = 0 \tag{16}$$

with

$$\begin{aligned}\alpha_i &= \mu_v R^{-1}_{ref|2D}S(\chi_{ref},\dot{\chi}_{ref})R_{ref|2D} + \alpha_v I \\ &\quad + R^{-1}_{ref|2D}\dot{S}(\chi_{ref},\dot{\chi}_{ref})R_{ref|2D} \\ &\quad + R^{-1}_{ref|2D}S^2(\chi_{ref},\dot{\chi}_{ref})R_{ref|2D} \\ &= \begin{bmatrix} \alpha_v - \chi^2_{ref} & \mu_v\dot{\chi}_{ref} + \ddot{\chi}_{ref} \\ -\mu_v\dot{\chi}_{ref} & \alpha_v - \chi^2_{ref} - \ddot{\chi}_{ref} \end{bmatrix}\end{aligned}$$

and

$$\begin{aligned}\mu_i &= 2R^{-1}_{ref|2D}S(\chi_{ref},\dot{\chi}_{ref})R_{ref|2D} + \mu_v I \\ &= \begin{bmatrix} \mu_v & 2\dot{\chi}_{ref} \\ -2\dot{\chi}_{ref} & \mu_v \end{bmatrix}\end{aligned}$$

The acceleration error vector in the inertial frame is written as

$$\ddot{\varepsilon}(t) = a - a_{ref} \tag{17}$$

where $a = (a_x, a_y)^T$ is the vehicle linear acceleration vector and $a_{ref} = (a_{x,ref}, a_{y,ref})^T$ its reference one. We stress that both vectors $\delta(t)$ and $\varepsilon(t)$ contain two components related to the planner position. Hence, using (16) and (17), the acceleration vector may be expressed as

$$a = -\mu_i\dot{\varepsilon}(t) - \alpha_i\varepsilon(t) + a_{ref} \tag{18}$$

Integrating equation (18), the planar velocity is

$$V = -\mu_i\varepsilon(t) - \alpha_i\int_{t_0}^{t}\varepsilon d\tau + V_{ref} + \Delta(t_0) \tag{19}$$

with initial term $\Delta(t_0) = V(t_0) + \mu_i\dot{\varepsilon}(t_0) - V_{ref}(t_0)$ and t_0 is the initial instant. Commonly, from a stationary flight ($V(t_0) = 0$) at the origin ($\varepsilon(t_0) = -P_{ref}(t_0)$), the quadrotor starts to follow the prescribed trajectory.

This new formulation has an integral action compared to (8), which gives more efficiency and cancel the steady-state errors. Then, we follow the same steps described in Section III-A, with

$$\begin{cases} \chi &= \dfrac{V_y}{|V_y|}\arccos\dfrac{V_x}{\|V\|_2} \\ \dot{\chi} &= \dfrac{V_y}{\|V_y\|}\left(\dfrac{a_xV_y - V_xa_y}{V_x^2 + V_y^2}\right) \end{cases}$$

IV. DYNAMIC MODEL AND NONLINEAR FLIGHT CONTROL

As the guidance law provides the velocities required to follow the prescribed trajectories, the flight controller is designed to ensure the velocity control. Thus, the quadrotor dynamic model should explicitly show the velocity term in the equations of motion.

A. Vehicle dynamics background

The quadrotor operates in two coordinate frames: the earth fixed frame $R_0(O_0,X,Y,Z)$ and the body frame $R_1(O_1,X_1,Y_1,Z_1)$. Let $\eta = (\phi,\theta,\psi)^T$ describes the orientation of the aerial vehicle (Roll, Pitch, Yaw) and $\zeta = (x,y,z)^T$ denotes the absolute position of the rotorcraft. For the current applications (inspection, coverage, etc.) that dont require aggressive maneuvers, the dynamic model of the quadrotor may be given by [9]

$$\ddot{\zeta} = \begin{bmatrix} u_1\dfrac{c\psi s\theta c\phi + s\psi s\phi}{m} \\ u_1\dfrac{s\psi s\theta c\phi - c\psi s\phi}{m} \\ -g + u_1\dfrac{c\theta c\phi}{m} \end{bmatrix} \tag{20}$$

$$\ddot{\eta} = \begin{bmatrix} \dot{\theta}\dot{\psi}\dfrac{I_y - I_z}{I_x} + J_r\dot{\theta}\Omega_r + \dfrac{u_2}{I_x} \\ \dot{\phi}\dot{\psi}\dfrac{I_z - I_x}{I_y} + J_r\dot{\phi}\Omega_r + \dfrac{u_3}{I_y} \\ \dot{\phi}\dot{\theta}\dfrac{I_x - I_y}{I_z} + \dfrac{u_4}{I_z} \end{bmatrix} \tag{21}$$

where $s_{(.)}$ and $c_{(.)}$ are abbreviations for $\sin(.)$ and $\cos(.)$ respectively, m the mass, g the gravity acceleration and u_1 the total thrust. $I = diag(I_x,I_y,I_z)$ is the diagonal inertia matrix, J_r denotes the rotors inertia and Ω a mixer of the rotors speeds, $\tau = (u_2,u_3,u_4)^T$ is the control torque. The quadrotor parameters are depicted in Table 1.

TABLE I

QUADROTOR PARAMETERS.

$m(kg)$	0.429	$I_y(kg.m^2)$	0.0029
$I_x(kg.m^2)$	0.0022	$I_z(kg.m^2)$	0.0048

B. Control oriented-model

According to our strategy of a non-holonomic way of navigation, the vehicle reaches any configuration in the space employing only the heading, the forward and the vertical motions. The heading is ensured by the control of the yaw while the forward motion is ensured by the pitch rotation.

Herein, we assume that the rolling angle is forced to be at the origin $\phi \to 0$ using a feedback controller as in [10].

Therefore, the overall dynamic model of quadrotor becomes

$$\ddot{\zeta} = \begin{bmatrix} u_1 \dfrac{c\psi s\theta}{m} \\ u_1 \dfrac{s\psi s\theta}{m} \\ -g + u_1 \dfrac{c\theta}{m} \end{bmatrix} \tag{22}$$

$$\ddot{\bar{\eta}} = \begin{bmatrix} \dfrac{u_3}{I_y} \\ \dfrac{u_4}{I_z} \end{bmatrix} \tag{23}$$

where $\bar{\eta} = (\theta, \psi)^T$.

From the two first equations of system (22), we define the following forward linear speed

$$\dot{V}_r = \frac{u_1 s\theta}{m} \tag{24}$$

where x and y dynamics are obtained directly as

$$\begin{cases} \ddot{x} &= \dot{V}_r c_\psi \\ \ddot{y} &= \dot{V}_r s_\psi \end{cases} \tag{25}$$

Therefore any location in the plane XY can be reached using the forward velocity and the heading angle. Based on equation (25) and by using systems (22) and (23), the reduced dynamic model is given by

$$\begin{cases} \dot{V}_r &= \dfrac{u_1 s\theta}{m} \\ \ddot{z} &= -g + u_1 \dfrac{c\theta}{m} \\ \ddot{\theta} &= \frac{u_3}{m} \\ \ddot{\psi} &= \frac{u_4}{m} \end{cases} \tag{26}$$

C. Control approach

The controller is herein designed to ensure the tracking of the desired trajectory along the three axes (x_r, y_r, z_r) and the yaw angle ψ_r and force the rolling angle to be at the origin (stabilization). The control structure is shown in Figure 5. The altitude and the yaw are controllers via u_1 and u_4 respectively using a simple feedback controller (see reference [10]).

The forward navigation in the plane XY is more challenging due to the fact that relates between the forward velocity and the pitch angle and it is considered as an underactuated subsystem. Therefore, *I&I* based control approach is proposed in order to deal with this problem of underactuation and ensures the asymptotic stability of the closed-loop of this subsystem.

1) Review of I&I based approach: The use of this approach (I&I) for stabilization of nonlinear systems was originated in [16]. First, we briefly recall, in the following, the definitions of the concepts of invariant manifold and immersion of systems.

Definition 1: *Consider the following autonomous system*

$$\dot{x} = f(x),\ y = h(x),\ \textit{with } x \in R^n \textit{and } y \in R^m \tag{27}$$

The manifold $M = \{x \in R^n | \phi(x) = 0\}$, is said to be invariant for $\dot{x} = f(x)$ if: $\phi(x(0)) = 0 \Rightarrow \phi(x(t))_{t \geq 0} = 0$ where $\phi(x)$ is a smooth flow.

Definition 2: *Immersion is a mapping of the initial state to another state-space of higher dimension. Consider, the following system*

$$\dot{\xi} = \alpha(\xi), \zeta = \beta(\xi),\ \textit{with } \xi \in R^p \textit{ and } \zeta \in R^m \tag{28}$$

System (28) is said to be immersed into system (27) if there exists a smooth mapping $\pi : R^p \to R^n$ which satisfies

- $x(0) = \pi(\xi(0))$
- $\beta(\xi_1) \neq \beta(\xi_2) \Rightarrow h(\pi(\xi_1)) \neq h(\pi(\xi_2))$

and such that
$f(\pi(\xi)) = \dfrac{\delta \pi}{\delta \xi}\alpha(\xi)$ *and* $h(\pi(\xi)) = \beta(\xi)$ *for all* $\xi \in R^p$

The major result of Immersion and Invariance is introduced by the following theorem:

Theorem 1: *Consider the system*

$$\dot{x} = f(x) + g(x)u \tag{29}$$

with a state vector $x \in R^n$, input $u \in R^m$ and $x^* \in R^n$ an equilibrium point to be stabilized.

Let $p < n$ and assuming existence of smooth mappings
$\alpha : R^p \to R^p$, $\pi : R^p \to R^n$, $\varsigma : R^n \to R^m$
$\phi : R^n \to R^{n-p}$, $\psi : R^{n \times (n-p)} \to R^m$
such that the following hold.

- **(C1)** *Target system*

The system $\dot{\xi} = \alpha(\xi)$ with state $\xi \in R^p$, has an asymptotically stable equilibrium at $\xi^* \in R^p$ and $x^* = \pi(\xi^*)$

- **(C2)** *Immersion condition*

For all $\xi \in R^p$, $f(\pi(\xi)) + g(\pi(\xi))\varsigma(\pi(\xi)) = \dfrac{\delta \pi}{\delta \xi}\alpha(\xi)$

- **(C3)** *implicit manifold*

The set identity $\{x \in R^p | \phi(x) = 0\} =$
$\{x \in R^n | x = \pi(\xi)$ *for some* $\xi \in R^p\}$ holds

- **(C4)** *Manifold attractively and trajectory boundedness*
All trajectories of the system

$$\dot{z} = \frac{\delta \phi}{\delta x}(f(x) + g(x)\psi(x,z))$$

$$\dot{x} = f(x) + g(x)\psi(x,z)$$

where $z = \phi(x)$, are bounded and satisfy $lim_{t\to\infty} z(t) = 0$. Then, x^* is asymptotically stable equilibrium of the closed-loop system $\dot{x} = f(x) + g(x)\psi(x,\phi(x))$ (For the theorem proof, see [16]).

2) Application of I&I: By choosing a state vector as $(x_1,x_2,x_3)^T = (V_r - V_{r_{ref}}, \theta, \dot{\theta})^T$. The subsystem in (26) becomes

$$\begin{cases} \dot{x}_1 &= \dfrac{u_1 s_{x2}}{m} - \dot{V}_{r_{ref}} \\ \dot{x}_2 &= x_3 \\ \dot{x}_3 &= \dfrac{u_3}{I_z} \end{cases} \tag{30}$$

I&I technique requires the selection of a target dynamical system. In order to avoid solving the partial differential equation **(C2)**, it has been proposed to choose the target system as a mechanical one parameterized in terms of potential and damping functions (see [17]). Thus, we define the target system as

$$\begin{cases} \dot{\xi}_1 &= \xi_2 \\ \dot{\xi}_2 &= \dfrac{\delta V(\xi_1)}{\delta \xi_1} - Q(\xi_1,\xi_2)\xi_2 \end{cases} \tag{31}$$

where the damping function, Q satisfies $Q(0,0) > 0$ and V the free potential scalar function, satisfies $\dfrac{\delta V(\xi_1)}{\delta \xi_1} = 0$. This ensures the asymptotic stability of the equilibrium point (ξ_1^*, ξ_2^*).

Remark 2: *The first condition **(C1)** is automatically satisfied because the target system is a priori defined.*

Remark 3: *Linear target dynamics is not, necessarily, suitable because of the constraints imposed by the physical structure and many systems are not linearizable by feedback. Our choice has been made for simplification reasons.*

By applying the immersion condition **(C2)**, we obtain: For small angles of pitch and all $\xi \in R^2$.

$$\bar{\pi} = \begin{bmatrix} \xi_1 \\ \dfrac{m}{u_1}(\xi_2 + \dot{V}_{r_{ref}}) \\ \pi(\xi_1,\xi_2) \end{bmatrix} \tag{32}$$

$$\pi(\xi_1,\xi_2) = \frac{m}{u_1}(\ddot{V}_{r_{ref}} - \acute{V}(\xi_1) - Q(\xi_1,\xi_2)\xi_2) \tag{33}$$

$$\frac{\varsigma(\pi(\xi))}{I_z} = \frac{\delta\pi(\xi_1,\xi_2)}{\delta\xi_1}\xi 2 + \frac{\delta\pi(\xi_1,\xi_2)}{\delta\xi_2}(-\ddot{V}(\xi_1) - Q(\xi_1,\xi_2)\xi_2) \tag{34}$$

From equations (33) and (34) we get $\pi(\xi_1,\xi_2)$ and the mapping $\varsigma(.)$ respectively. It is easy to define the manifolds of **(C3)** and can be implicitly described by

$$\phi(x) \triangleq x_3 - \pi(x_1,x_2) = 0 \tag{35}$$

To make the manifold attractive and satisfying **(C4)**, the manifold dynamics is given as

$$\begin{aligned} &\dot{Z} = (\dot{x}_3 - \dot{\pi}(x_1,x_2)) \\ &= (\frac{\psi(x,Z)}{I_z} - \frac{\delta\pi}{\delta x_1}(\frac{u_1 x_1}{m} - \dot{V}_{r_{ref}}) - \frac{\delta\pi}{\delta x_2}x_3) \end{aligned} \tag{36}$$

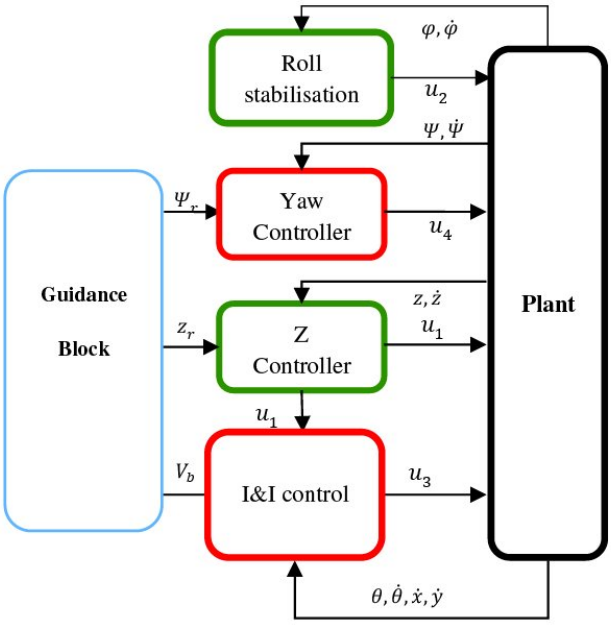

Fig. 5. Controlled system Architecture.

where $Z = \phi(x)$
Taking

$$\dot{Z} = -\lambda Z \tag{37}$$

Hence selecting λ as positive constants exponentially drives Z to zero. The resulting controller then takes the form

$$\begin{aligned} \psi(x,\phi(x)) \quad &= \frac{\delta\pi}{\delta x_1}(\frac{u_1 x_2}{m} - \dot{V}_{r_{ref}}) + \frac{\delta\pi}{\delta x_2}x_3 \\ &-\lambda(x_3\pi(x_1,x_2)) \end{aligned} \tag{38}$$

Remark 4: *It is easy to verify that the control law satisfies $\psi(x,0) = \varsigma(\pi)$ with $\varsigma(\pi)$ defined by (34), thus the immersion condition **(C2)** is satisfied.*

Proposition 1: *For any mapping satisfying (35), such that conditions **(C3)** and **(C4)** hold using appropriate V and Q, the equilibrium of system (30) in closed loop via controller (38) is asymptotically stable.*

The design procedure is conducted by choosing the functions V and Q. For the sake of simplicity, we select $V = \frac{1}{2}k_V\xi_1^2$ and $Q = K_Q$ with k_v, $k_Q > 0$
Then

$$\pi(x_1,x_2) = -\frac{m}{u_1}k_V x_1 - k_Q x_2 \tag{39}$$

Finally, doing some computations, the control effort for system (30) is expressed as

$$\begin{aligned} u_3 \quad &= -\frac{m}{u_1}k_V x_1 - (k_V x_2 + \lambda k_Q)x_2 - (k_Q + \lambda)x_3 \\ &(\lambda\frac{m}{u_1}k_Q + k_V\frac{m}{u_1})\dot{V}_{r_{ref}} + \lambda\frac{m}{u_1}\ddot{V}_{r_{ref}} \end{aligned} \tag{40}$$

where λ, k_Q and k_V are positive constants.

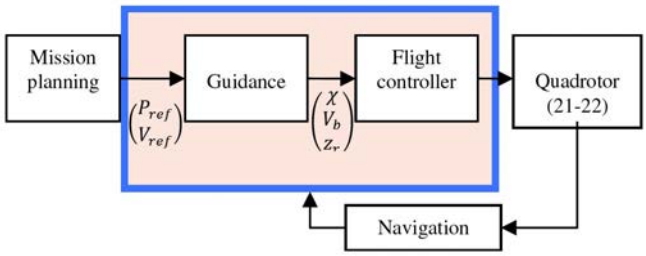

Fig. 6. GNC global structure.

V. NUMERICAL RESULTS

Now, since we have completed equations describing the dynamics of the system, the guidance law and the equation of the flight control law, we can design a simulation environment in order to test and view the results of various signals. The guidance and control parameters are tuned by minimizing the following objective function using Genetic Algorithms (GA).

$$O_f = \frac{1}{t_1 - t_0} \int_{t_0}^{t_1} \varepsilon^T \varepsilon d\tau \tag{41}$$

where t_1 and t_0 are the final and the initial times respectively, $\varepsilon(\tau)$ is the tracking error of the considered output. They are given by

- Guidance laws: $\lambda_v = 5$, $\alpha_v = 5$ and $\mu_v = 0.5$
- Flight control law: $\lambda = 30$, $k_V = 7$ and $k_Q = 3$

The reference trajectory is described by the inertial position vector P_{ref} and the velocity vector V_{ref} . They are considered as inputs for the guidance module. Using these inputs, the guidance module generate the adequate signals in order to ensure the non-holonomic like navigation way that are considered as inputs of the flight control system. They are the heading angle χ and the linear speed V_b as well as the altitude. The flight controller sends the required inputs to the quadrotor represented by the overall dynamics (20-21). The global structure of the Guidance, Navigation and Control (GNC) loop is depicted in Figure 6. The tests have been performed in both cases in absence and presence of lateral wind with speed mean value of (1, 5, 10) m/sec.

Firstly, we investigate the effectiveness of the proposed G&C system in the ideal case. As example of scenario, the tracking errors of the absolute position and the heading angle are depicted in Figure 7. Finally, the 3D performed trajectory is shown in Figure 8. Clearly, the vehicle G&C system ensures a good tracking of the reference trajectory with good accuracy (see Figure 7). These observations may be confirmed by the 3D trajectory displayed in Figure 8 where the prescribed reference trajectory and the vehicle trajectory are quite consistent.

Secondly, we check the effectiveness of the G&C system with respect to the wind. Therefore, in the presence of lateral wind of mean values (1, 5, 10) m/sec, we illustrate in Figure 9 the 3D trajectory of the vehicle.

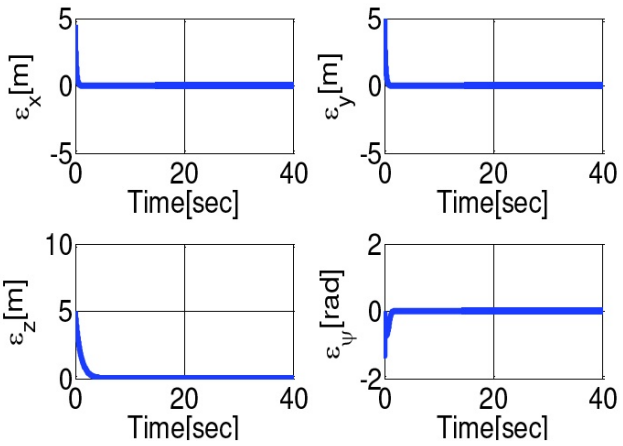

Fig. 7. Tracking errors of the absolute position and the heading angle (without wind).

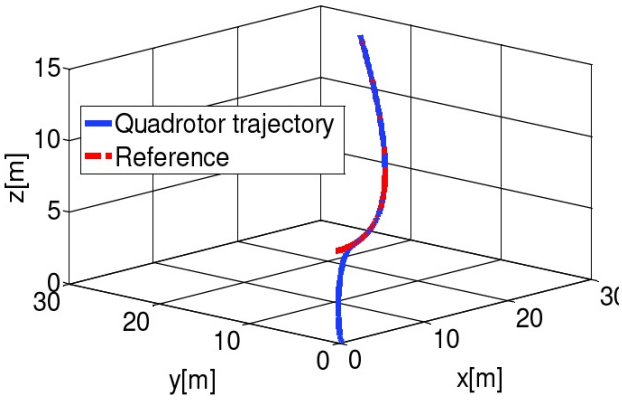

Fig. 8. 3D trajectory (without wind).

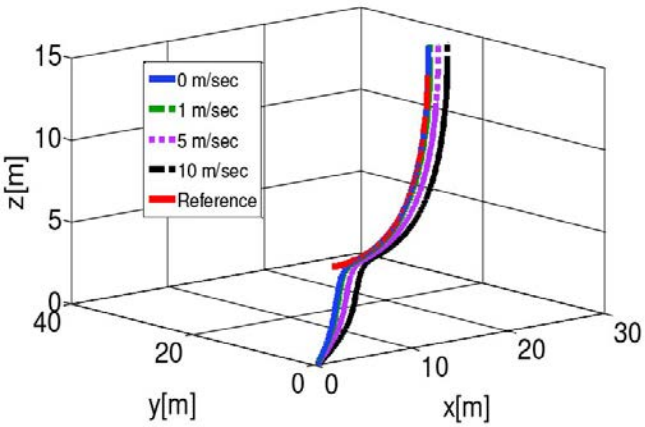

Fig. 9. 3D trajectory (with wind).

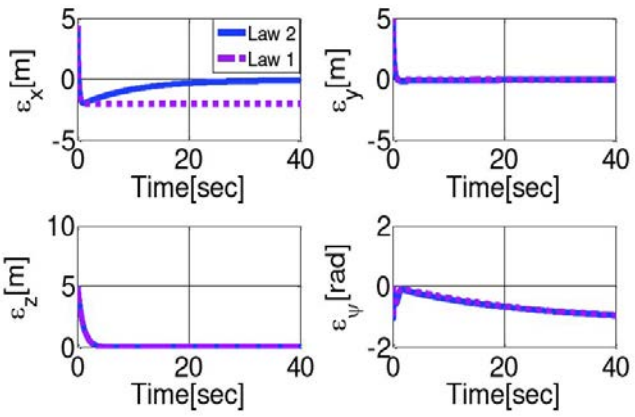

Fig. 10. Tracking errors of the absolute position and the heading angle in presence of wind of 10 m/sec.

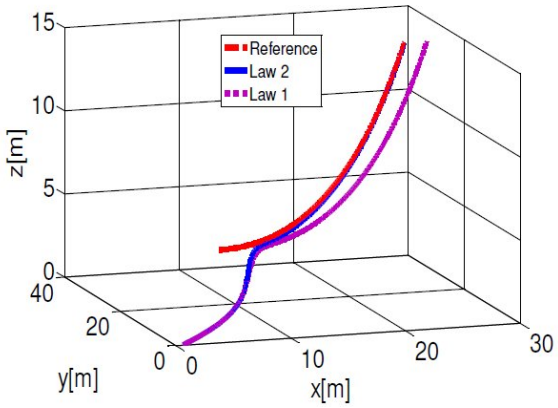

Fig. 11. 3D trajectory in presence of wind of 10 m/sec.

The quadrotor manages to follow the prescribed reference trajectory but it exhibits much more deviation proportionally to the speed of the wind. Therefore, first guidance law (8) is not able to correct the trajectory affected by the wind where a clear steady-state is created.

For the sake of improvement an integral action is introduced by using guidance law (19). The tracking errors using laws (8) and (19) in presence of wind whose speed is of 10 m/sec are shown in Figure 10. The 3D trajectories are shown in Figure 11. Notice that the same controller and guidance law parameters are used. Figure 10 and Figure 11 show that the use of the second law raises the performance of the technique where the steady state is clearly reduced. For the remaining cases, the Integral Square Error (ISE) given by

$$ISE = \frac{1}{t_f - t_0} \int_{t_0}^{t_f} \varepsilon(t)^T \varepsilon(t) dt \tag{42}$$

is computed for the overall trajectory and tabulated in Table 2. One may observe that the method based on the second order law is shown to be the best one in case of windy environment. The first law leads to quite similar performance

TABLE II

SQUARE TRACKING ERROR.

Wind mean speed $[m/sec]$	***Law 1 (8)***	***Law 2 (19)***
0	0.00439	0.00440
1	0.00476	0.00447
5	0.01416	0.00569
10	0.04379	0.00946

in the ideal case.

VI. CONCLUSION

This paper has treated the subject of guidance related to motion behavior in a 2D plane and a 3D space. Two alternatives of guidance law are developed that allows the quadrotor to follow any path as well as a fixed wing UAV (non-holonomic like-navigation). The first guidance law can perform the task with good features in the case without wind but with poor capabilities to cancel the steady-state errors. Therefore, the second law that incorporates an integral action and uses the acceleration instead of the velocities exhibits good results even in presence of wind. The flight controller, based on I&I approach, globally exhibits good performance. Simulation results are shown supporting these claims.

REFERENCES

[1] J. A. Guerrero and Y. Bestaoui, "Uav path planning for structure inspection in windy environments," *Journal of Intelligent & Robotic Systems*, vol. 69, no. 1-4, pp. 297–311, 2013.

[2] Y. Bouzid, Y. Bestaoui, and H. Siguerdidjane, "Two-scale geometric path planning of quadrotor with obstacle avoidance: First step toward coverage algorithm," in *2017 11th International Workshop on Robot Motion and Control (RoMoCo)*, Jul. 2017, pp. 166–171.

[3] C. Goerzen, Z. Kong, and B. Mettler, "A survey of motion planning algorithms from the perspective of autonomous uav guidance," *Journal of Intelligent and Robotic Systems*, vol. 57, no. 1-4, p. 65, 2010.

[4] D. Mellinger, N. Michael, and V. Kumar, "Trajectory generation and control for precise aggressive maneuvers with quadrotors," *The International Journal of Robotics Research*, vol. 31, no. 5, pp. 664–674, 2012.

[5] D. R. Nelson, D. B. Barber, T. W. McLain, and R. W. Beard, "Vector field path following for small unmanned air vehicles," in *American Control Conference, 2006*. IEEE, 2006, pp. 7–pp.

[6] J. Osborne and R. Rysdyk, "Waypoint guidance for small uavs in wind," in *Infotech@ Aerospace*, 2005, p. 6951.

[7] M. Breivik and T. I. Fossen, "Principles of guidance-based path following in 2d and 3d," in *Decision and Control, 2005 and 2005 European Control Conference. CDC-ECC'05. 44th IEEE Conference on*. IEEE, 2005, pp. 627–634.

[8] P. Sujit, S. Saripalli, and J. B. Sousa, "Unmanned aerial vehicle path following: A survey and analysis of algorithms for fixed-wing unmanned aerial vehicless," *IEEE Control Systems*, vol. 34, no. 1, pp. 42–59, 2014.

[9] S. Bouabdallah, A. Noth, and R. Siegwart, "Pid vs lq control techniques applied to an indoor micro quadrotor," in *Intelligent Robots and Systems, 2004.(IROS 2004). Proceedings. 2004 IEEE/RSJ International Conference on*, vol. 3. IEEE, 2004, pp. 2451–2456.

[10] Y. Bouzid, H. Siguerdidjane, and Y. Bestaoui, "Flight control boosters for three-dimensional trajectory tracking of quadrotor: Theory and experiment," *Proceedings of the Institution of Mechanical Engineers, Part I: Journal of Systems and Control Engineering*, p. 0959651818757159, Mar. 2018. [Online]. Available: https://doi.org/10.1177/0959651818757159

[11] Y. Bouzid, H. Siguerdidjane, Y. Bestaoui, and M. Zareb, "Energy based 3d autopilot for vtol uav under guidance & navigation constraints," *Journal of Intelligent & Robotic Systems*, vol. 87, no. 2, pp. 341–362, 2017.

[12] Y. Bouzid, H. Siguerdidjane, and Y. Bestaoui, "Nonlinear internal model control applied to VTOL multi-rotors UAV," *Mechatronics*, vol. 47, pp. 49–66, Nov. 2017. [Online]. Available: http://www.sciencedirect.com/science/article/pii/S0957415817301046

[13] J. Escareno, L. Garcia, C. Chauffaut, V. Santibañez, and R. Lozano, "Nonholomic-like corridor navigation of a quad-rotor mav using optical flow," *IFAC Proceedings Volumes*, vol. 45, no. 4, pp. 248–253, 2012.

[14] J. Escareño, S. Salazar, H. Romero, and R. Lozano, "Trajectory control of a quadrotor subject to 2d wind disturbances," *Journal of Intelligent & Robotic Systems*, vol. 70, no. 1-4, pp. 51–63, 2013.

[15] Y. Bouzid, Y. Bestaoui, and H. Siguerdidjane, "Quadrotor-UAV optimal coverage path planning in cluttered environment with a limited onboard energy," in *2017 IEEE/RSJ International Conference on Intelligent Robots and Systems (IROS)*, Sep. 2017, pp. 979–984.

[16] A. Astolfi and R. Ortega, "Immersion and invariance: A new tool for stabilization and adaptive control of nonlinear systems," *IEEE Transactions on Automatic control*, vol. 48, no. 4, pp. 590–606, 2003.

[17] J. Acosta, R. Ortega, A. Astolfi, and I. Sarras, "A constructive solution for stabilization via immersion and invariance: The cart and pendulum system," *Automatica*, vol. 44, no. 9, pp. 2352–2357, 2008.